the growth curves (i.e., $L'_{ri}/T'_{ri} = [L_{ri}/T_{ri}]/[L_{r4}/T_{r4}]$, where L'_{ri}/T'_{ri} denotes the re-normalised sensitivity-corrected regenerative dose signals), and the additional regenerative dose D_r required for determining the gSGC D_e was set equal to $0.8D_n$. The average dose response curve (re-normalised dose response curve) was fitted using a single saturating exponential function in order to calculate the SGC (gSGC) D_e.

We obtained decay rates for the fast and medium components by deconvoluting simulated decay curves into two first-order exponential decaying components as well as a constant component using the decomp() function from the R package numOSL. Similarly, the characteristic saturation dose D_0 values were obtained by fitting the growth curves with a single saturating exponential model, using the fitGrowth() function from the R package numOSL. Typical resultant variations in simulated natural dose signal intensity, ratio of fast to medium decay rates, and characteristic saturation dose D_0 are demonstrated in Fig. 1A, B, and C respectively, for a given dose of 240 Gy. The RSD values for the mean of these parameters are of the order of 1–2%, which is generally within the range of typical experimental OSL data.

Fig. 2A and B shows the sensitivity-corrected regenerative dose signals L_{ri}/T_{ri} and their re-normalised counterpart L'_{ri}/T'_{ri} correspondingly, for 3000 randomly simulated growth curves for a given dose of 240 Gy. These figures demonstrate that the re-normalisation procedure used in the gSGC procedure can reduce significantly the scatter of the sensitivity-corrected regenerative dose signals. Specifically, if we denote the fifth sensitivity-corrected regenerative dose signal before and after re-normalisation as L_{r5}/T_{r5} and L'_{r5}/T'_{r5}, respectively, then the RSD in L_{r5}/T_{r5} is 6.18%. The RSD for L'_{r5}/T'_{r5} reduces to 2.73% if the third regenerative dose D_{r3} (L_{r3}/T_{r3}) is used to re-normalise the growth curve (i.e., $L'_{ri}/T'_{ri} = [L_{ri}/T_{ri}]/[L_{r3}/T_{r3}]$) (Fig. 2A). The RSD for L'_{r5}/T'_{r5} is further reduced to 1.15% if the fourth regenerative dose D_{r4} (L_{r4}/T_{r4}) is used for re-normalisation (i.e., $L'_{ri}/T'_{ri} = [L_{ri}/T_{ri}]/[L_{r4}/T_{r4}]$) (Fig. 2B).

Fig. 2C and D shows the simulated D_e distributions obtained from the SGC and gSGC methods respectively, for a given dose of 240 Gy, visualized by a simplified (pseudo) radial plot (Galbraith, 1988) implemented using function psRadialPlot() from the R

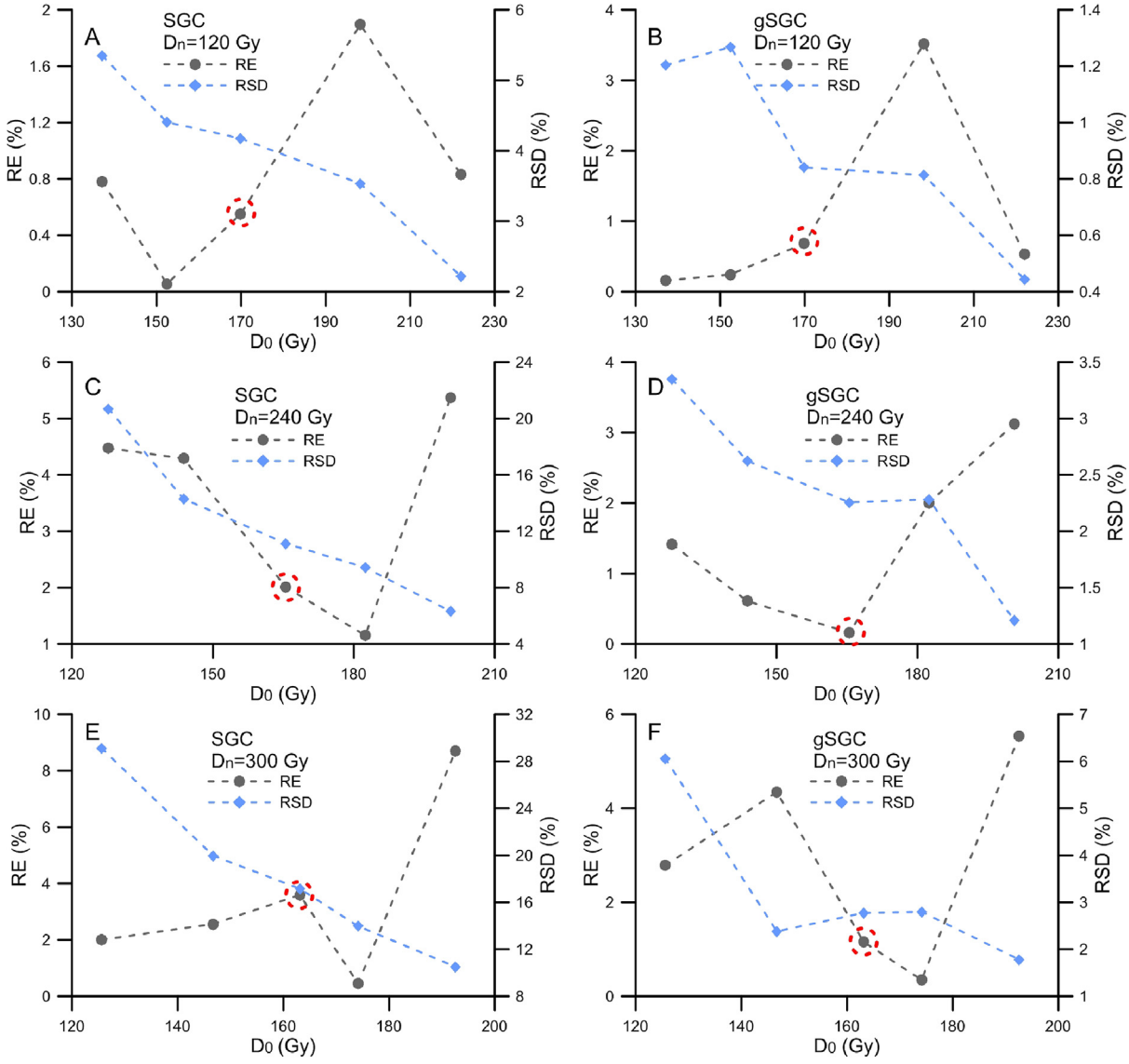

Fig. 6. Variation of RSD and RE of SGC and gSGC D_e estimates with D_0 (N_8) for various given doses D_n. Each data point was based on 500 versions of simulation. The data points encircled by dashed circles denote the RE of D_e estimates simulated using the default N_8 value of 1×10^{11} cm^{-3}.

package numOSL. The recovered average D_e values using the SGC and gSGC methods are 244.82 Gy and 239.62 Gy respectively. The standard deviations of the 500 model variants calculated from the SGC and gSGC methods are 27.25 Gy and 5.40 Gy respectively. Accordingly, the RSD for the SGC and gSGC D_e estimates are 11.13% and 2.25%, respectively. The over-dispersion values (Galbraith et al., 1999) for the recovered SGC and gSGC D_e distributions are $9.14 \pm 0.39\%$ and $0.21 \pm 0.16\%$ respectively. These simulation results suggest that the gSGC method can greatly improve the precision of D_e estimates over the SGC method.

Fig. 3 shows a comparison of recovered D_e estimates obtained by the SGC and gSGC methods for given doses D_n in the range 30–300 Gy. It can be observed from Fig. 3 that for given doses less than 120 Gy the differences in RSD and RE between SGC and gSGC D_e values are smaller than 4%. The difference in RSD between D_e estimates obtained from the two methods increases substantially when the given dose exceeds 120 Gy. However, the overall differences in RE are smaller than 3% for investigated dose values up to 300 Gy. The simulation indicates that the gSGC method can significantly improve the precision of D_e estimates compared to the SGC method, though the difference in accuracy between D_e estimates obtained from the two methods is not very significant for given dose less than 210 Gy.

3. Investigation of factors influencing the reliability of the SGC and gSGC D_e estimates

In this section, we investigate the effect of various parameters on the reliability of the SGC and gSGC D_e estimates; these parameters are the characteristic saturation dose D_0 of a growth curve, the number of aliquots used for SGC and gSGC establishment, the size of the additional regenerative dose D_r (L_r/T_r) used for re-normalising the sensitivity-corrected natural dose signal, and the size of the regenerative dose D_{ri} (L_{ri}/T_{ri}) used for re-normalising the growth curves. It deserves to be pointed out that it is not always the case that the sensitivity-corrected natural dose signal and the growth curves should be re-normalised by a regenerative dose of the same magnitude (i.e., D_r may not be equal to D_{ri}) during gSGC D_e estimation. A researcher may use an additional regenerative dose D_r that is different in magnitude from all of the D_{ri} values but

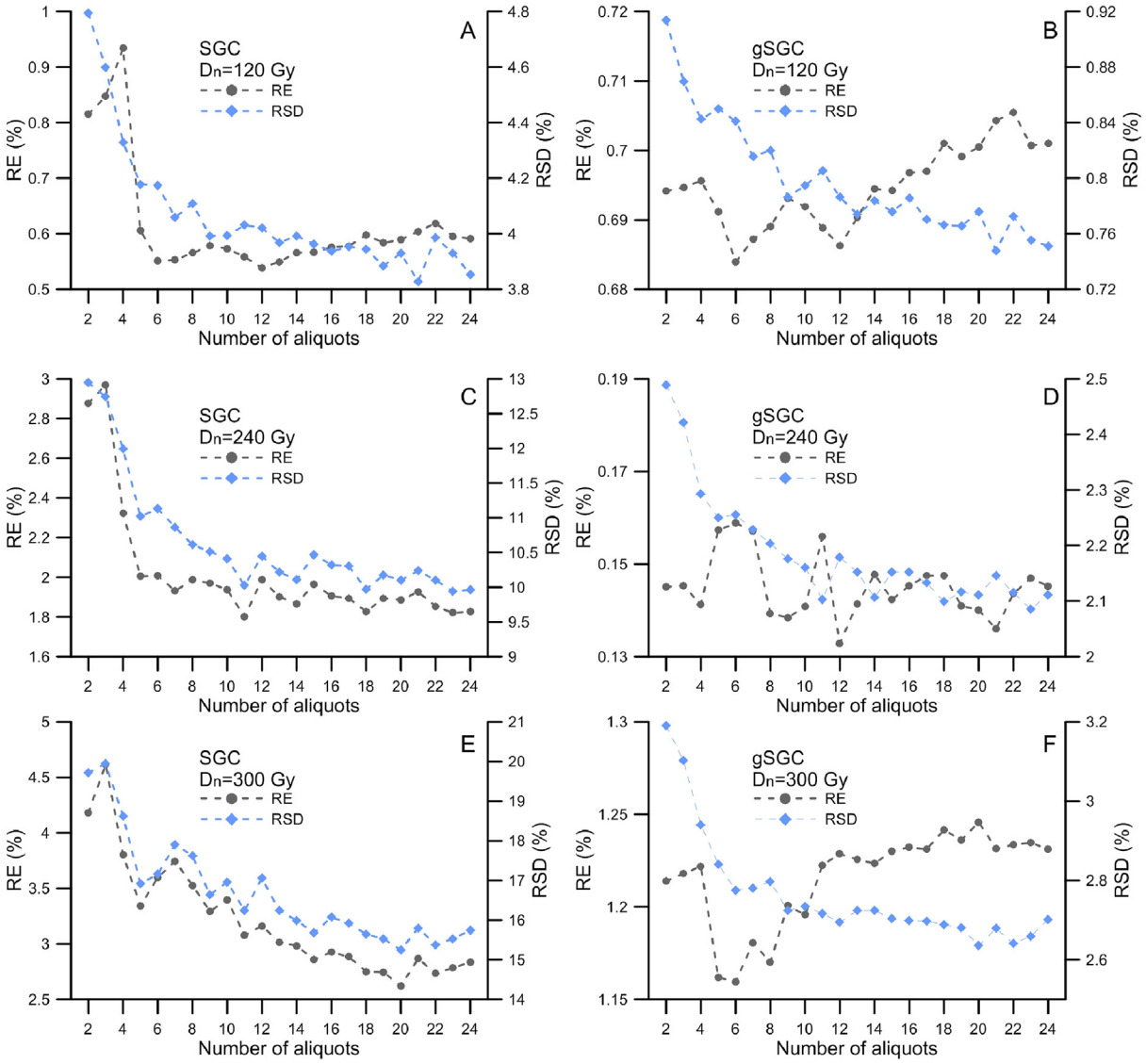

Fig. 7. Variation of RSD and RE of SGC and gSGC D_e estimates with the number of aliquots used to establish the SGC and gSGC for various given doses D_n. The investigated number of aliquots ranges from 2 to 24 with an interval of 1. Each data point was based on 500 model variants.

close in size to the given dose D_n for re-normalising the sensitivity-corrected natural dose signal, in order to improve the precision of calculated gSGC D_e.

We simulated the dose recovery experiments using different values for the kinetic parameter N_8 (i.e., the total concentration of holes for the "luminescence center" L), in order to change the characteristic saturation dose D_0 of the generated random growth curves. It was found in the simulations that as the value of the parameter N_8 is increased in the model, the sensitivity of the simulated signals will also increase. Specifically larger values of N_8 yield greater signal intensity for both the regenerative dose OSL response L_{ri} and for the test dose OSL response T_{ri}. Furthermore, simulated L_{ri} and T_{ri} with greater signal intensity result in simulated growth curves which tend to saturate at lower doses. Consequently, a larger N_8 value results in smaller D_0 values for the growth curves, and vice versa.

Fig. 4 illustrates random growth curves and sensitivity-corrected given (natural) dose signals simulated using the SGC method. Fig. 4A, C, and E show respectively distributions of 3000 variants of random growth curves simulated using N_8 values of 1×10^6, 1×10^{11}, and 1×10^{16} cm^{-3} for a given dose $D_n = 240$ Gy. The corresponding characteristic saturating dose D_0 are 200.60 ± 17.00 Gy, 165.53 ± 15.81 Gy, and 127.76 ± 13.87 Gy, respectively. It suggests that the variability in growth curves is insignificant for regenerative dose below 100 Gy, and it increases substantially at larger regenerative doses. This also implies that the observed larger uncertainty in SGC D_e estimates of Fig. 3 is mainly caused by the large variability of growth curves for regenerative doses above 100 Gy; it is concluded that the SGC method cannot effectively eliminate the between-aliquot scatter of different growth curves.

Fig. 4.B, D, and F illustrate the effect of D_0 values on the distributions of sensitivity-corrected given (natural) dose signal L_n/T_n. The RSD of L_n/T_n for low, intermediate and high N_8 values are 2.7%, 4.3%, and 5.7% respectively, suggesting that the variability of L_n/T_n increases as the D_0 values decrease. The uncertainty of resultant SGC D_e estimates also increases as D_0 decreases. These results are consistent with Fig. 4A, C, and E, which demonstrates that the RSD of sensitivity-corrected regenerative dose signals L_{ri}/T_{ri} increases as D_0 decreases.

Fig. 5 shows the same data as in Fig. 4, with the data re-normalised using the gSGC method. In Fig. 5A, C, and E, the simulated growth curves were re-normalised using the fourth regenerative dose D_{r4} (L_{r4}/T_{r4}) (i.e., $L'_{ri}/T'_{ri} = [L_{ri}/T_{ri}]/[L_{r4}/T_{r4}]$). In Fig. 5B, D, and F, the simulated sensitivity-corrected given (natural) dose signal was re-normalised using an additional regenerative dose D_r (L_r/T_r) and the established gSGC according to Eq. (10) of Li et al. (2015a). We denote this re-normalised sensitivity-corrected natural dose signal by L'_n/T'_n. It can be seen from Fig. 5A, C, and E that D_0 values of the re-normalised growth curves are the same as those in Fig. 4A, C, and E, suggesting that the re-normalisation procedure will not affect the D_0 values of the growth curves.

It can be observed from contrasting Figs. 4 and 5 that the variability of growth curves decreased significantly after applying the re-normalisation procedure. The scatter in re-normalised growth curves is not only small for regenerative dose less than 100 Gy but also less significant for larger regenerative doses (Fig. 5), in comparison to that illustrated in Fig. 4. The RSD of L'_n/T'_n for low, intermediate, high N_8 values are 0.7%, 1.1%, and 1.3% respectively. These values are significantly smaller than those obtained in Fig. 4 for their un-normalised counterparts. A comparison between Figs. 4 and 5 clearly illustrates why the uncertainty of D_e estimates obtained from the gSGC method is significantly smaller than the ones obtained from the SGC method. The gSGC method reduces the variation in growth curves, to a much greater extent than the SGC method.

Fig. 6 demonstrates the variation of RSD and RE of SGC and gSGC D_e estimates with the D_0 (N_8). It can be seen from the scales of the y-axes that generally both the RSD and RE of D_e estimates obtained from the gSGC method are smaller than their SGC counterpart (except in the $D_n = 120$ Gy case). There is no obvious correlation between the RE of SGC and gSGC D_e estimates and the characteristic saturation dose D_0 for various given doses. In most cases, the D_e estimates yield lower RE (smaller than 4%) using moderate D_0 values corresponding to the default N_8 value of 1×10^{11} cm^{-3} used in the model of Bailey (2001). A monotonic decrease in the RSD of SGC and gSGC D_e estimates with increased D_0 values was observed in almost all cases. This is because the scatter in both the sensitivity-corrected natural dose signal and in the sensitivity-corrected regenerative dose signals (as well as their re-normalised counterparts) decreases with the increase in D_0 values, as was illustrated in Figs. 4 and 5.

During the application of the SGC (gSGC) method, the SGC (gSGC) used for D_e determination is usually established from the average of a number of growth curves (re-normalised growth

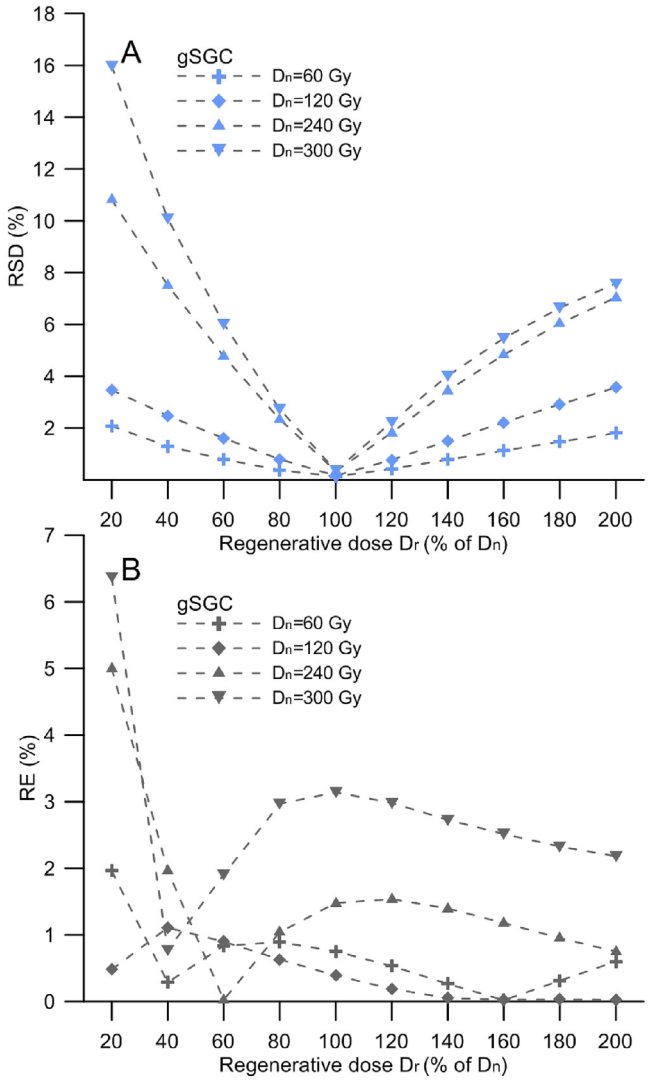

Fig. 8. Variation of RSD (A) and RE (B) of gSGC D_e estimates with the size of the additional regenerative dose D_r (L_r/T_r) used to re-normalise the sensitivity-corrected natural dose signal for various given doses D_n. D_r ranges from $0.2D_n$ to $2D_n$ with a step of $0.2D_n$. Each data point was based on 500 model variants. Note that the scales of x-axes are expressed as percent of the given dose D_n.

curves) from different aliquots. Fig. 7 demonstrates the variation of RSD and RE of SGC and gSGC D_e estimates with the number of aliquots used for SGC and gSGC establishment. It can be observed from Fig. 7 that increasing the number of aliquots improves the precision of SGC and gSGC D_e estimates. This is because of overall improvements of the statistics; the uncertainty of the average dose response curve (re-normalised dose response curve) used to determine the SGC (gSGC) D_e values will decrease by using more aliquots in the procedure.

Using more aliquots also improves the accuracy of SGC D_e estimates, as illustrated in Fig. 7A, C, and E. However, it seems that the accuracy of gSGC D_e estimates is not sensitive to the variation of number of aliquots, and shows a random variation pattern. This may imply that in the gSGC method the number of aliquots used for gSGC establishment is not a major factor controlling the accuracy of D_e estimates.

In most cases both the RSD and RE of D_e estimates obtained from the gSGC method are significantly smaller than their SGC counterpart. An exception is that the RE of gSGC D_e estimates is slightly larger than that obtained by the SGC method for a given dose $D_n = 120$ Gy when the number of aliquots exceed 6, as demonstrated in Fig. 7A and B. This may suggest that when applying the gSGC method to determining D_e values smaller than 120 Gy, the gain in accuracy is not obvious compared to the SGC method. This is consistent with Fig. 3, which suggests that the difference in RE between the two methods is less than 1% for given dose up to 210 Gy.

The re-normalisation procedure used in the gSGC method requires a sensitivity-corrected regenerative dose signal to be measured, in addition to the sensitivity-corrected natural dose signal. These signals are used in combination with the established gSGC in order to determine the gSGC D_e value. Fig. 8 plots the RSD and RE of gSGC D_e estimates against the size of the additional regenerative dose D_r. The results indicate that the size of the regenerative dose D_r (L_r/T_r) used for re-normalising the sensitivity-corrected natural dose signal can significantly affect the precision of gSGC D_e estimates (Fig. 8A). Recovered gSGC D_e values for different given doses are of low RSD (smaller than 4%), if the additional regenerative dose D_r varies between $0.8D_n$ and $1.2D_n$. The gSGC D_e estimates have the lowest RSD when the additional regenerative dose is set equal to the given dose (i.e., if $D_r = D_n$). The RSD of gSGC D_e estimates become increasingly larger with the increase in the difference between D_n and D_r. The simulation validates the conclusion drawn by Li et al. (2015a) that the chosen additional regenerative dose should be as close as possible in size to that of the natural dose, in order to minimize the scatter in the re-normalised sensitivity-corrected natural dose signal L'_n/T'_n.

However, there is no obvious correlation between the accuracy of gSCG D_e estimates and the size of the additional regenerative dose D_r (L_r/T_r) (Fig. 8B). In addition, the best accuracy of gSGC D_e estimates does not correspond to an additional regenerative dose that is equal in size to the given dose. Interestingly, for given doses

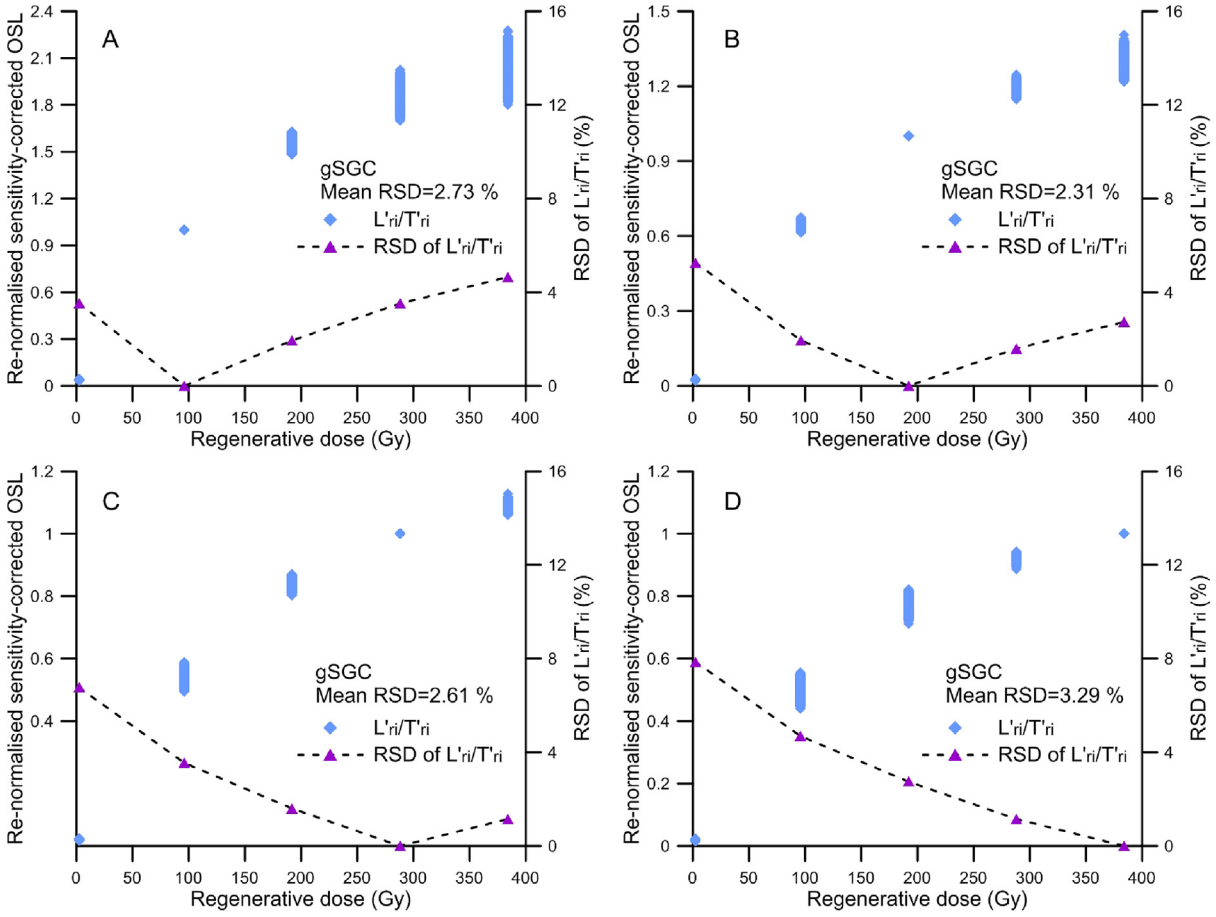

Fig. 9. Variation of re-normalised sensitivity-corrected regenerative dose signals L'_{ri}/T'_{ri} with the size of regenerative dose D_{ri} (L_{ri}/T_{ri}) used for growth curve re-normalisation for a given dose of 240 Gy. (A), (B), (C), and (D) were re-normalised using regenerative dose values of $0.4D_n$, $0.8D_n$, $1.2D_n$, and $1.6D_n$ Gy (Table 2), respectively. Each subplot was based on 3000 randomly simulated growth curves.

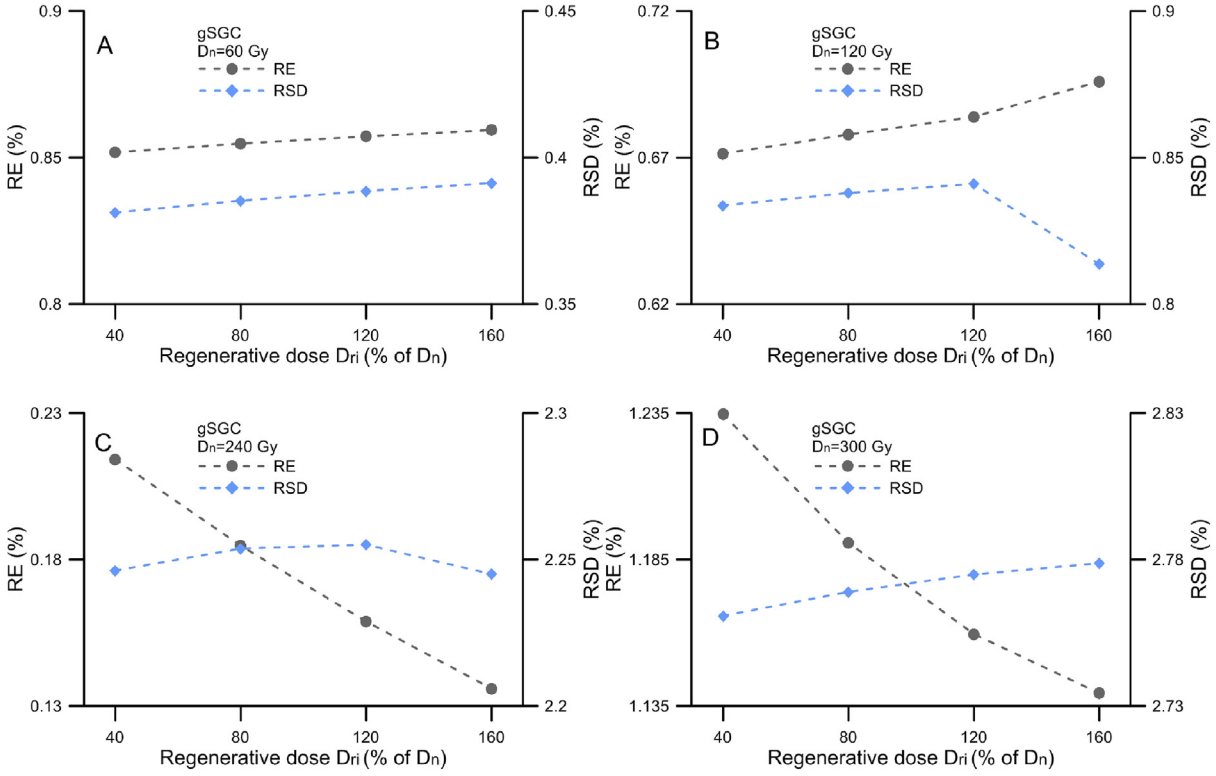

Fig. 10. Variation of RSD and RE of gSGC D_e estimates with the size of the regenerative dose D_{ri} (L_{ri}/T_{ri}) used for growth curve re-normalisation for various given doses D_n. The four regenerative dose values used for re-normalisation are $0.4D_n$, $0.8D_n$, $1.2D_n$, and $1.6D_n$ Gy (Table 2). Each data point was based on 500 model variants. Note that the scales of x-axes are expressed as percent of the given dose D_n.

$D_n = 60$ Gy and $D_n = 120$ Gy, gSGC D_e estimates have the lowest RE when the additional regenerative dose D_r is equal to $1.6D_n$. For given dose $D_n = 240$ Gy and $D_n = 300$ Gy, gSGC D_e estimates have the lowest RE when the additional regenerative doses are set equal to $0.6D_n$ and $0.4D_n$, respectively. This suggests that the correlation between accuracy of gSGC D_e estimates and the size of additional regenerative doses used for re-normalisation is complex, and does not follow a specific pattern. It seems that lower RE is obtainable when smaller additional regenerative dose is used for re-normalisation of a larger given dose, and vice versa.

Li et al. (2015a) illustrated how the choice of the size of the regenerative dose D_{ri} (L_{ri}/T_{ri}) used for re-normalising the growth curves affects the extent of variation between aliquots (growth curves). During the simulation it was observed that the scatter in re-normalised growth curves varies slightly when different regenerative doses D_{ri} (L_{ri}/T_{ri}) were used for re-normalisation of the growth curves, as demonstrated in Fig. 9 for a given dose of 240 Gy. The resultant mean RSD of L'_{ri}/T'_{ri} were 2.73%, 2.31%, 2.61%, and 3.29% respectively if regenerative dose values of $0.4D_n$, $0.8D_n$, $1.2D_n$, and $1.6D_n$ Gy were used for growth curve re-normalisation. Fig. 10 shows the influences of the size of the regenerative dose D_{ri} (L_{ri}/T_{ri}) used for re-normalising the growth curves on the RSD and RE of gSGC D_e estimates for different given doses. It can be observed from Fig. 10 that there is no obvious variation trend for the RSD or RE of gSGC D_e estimates with the regenerative dose D_{ri} (L_{ri}/T_{ri}) used for re-normalisation. It can also be seen from the scales of y-axes in Fig. 10 that the influence of the regenerative dose sizes used for growth curve re-normalisation on the RSD and RE of gSGC D_e estimates is relatively insignificant. For all the four investigated regenerative dose points, the variations in RSD and RE of gSGC D_e estimates are less than 0.1%.

4. Conclusions

The comprehensive quartz model of Bailey (2001) was used in this paper to simulate dose recovery experiments, in order to assess the intrinsic precision and accuracy of the SGC and gSGC D_e estimates. The simulation results show that the gSGC method can significantly improve the precision of D_e estimates compared to the SGC method. It suggests that the difference in RE between the SGC and gSGC methods is less than 3% for investigated doses up to 300 Gy. However, the RSD of gSGC D_e estimates was significantly smaller than that of SGC D_e estimates. The simulation experiments validate that the between-aliquot scatter in growth curves can be effectively eliminated by using the re-normalisation procedure employed in the gSGC method.

Several factors which may be affecting both the intrinsic precision and accuracy of the two methods were investigated. The simulation results suggest that:

(1) The precision of SGC and gSGC D_e estimates can be improved if growth curves with larger characteristic saturation dose D_0 are used.
(2) Using a larger number of aliquots (growth curves) to establish the SGC can improve both precision and accuracy of SGC D_e estimates. However, though the precision of gSGC D_e estimates also improves with the increase in the number of aliquots used, it seems that the accuracy of gSGC D_e estimates is not sensitive to variations in the number of aliquots.
(3) The precision of gSGC D_e estimates is very sensitive to the size of the additional regenerative dose D_r (L_r/T_r) used for re-normalising the sensitivity-corrected natural dose signal.

Better precision is obtainable if the additional regenerative dose D_r used for re-normalisation is close in size to the given dose D_n.

(4) Both the precision and accuracy of gSGC D_e estimates are insensitive to the size of the regenerative dose D_{ri} (L_{ri}/T_{ri}) used for re-normalising the growth curves. For doses up to 300 Gy, the variations in RSD and RE of gSGC D_e estimates are less than 0.1% when different regenerative dose sizes D_{ri} were used for re-normalisation.

The simulation results presented in this study demonstrate that the gSGC method is almost always intrinsically more precise than the SGC method given that a proper size of additional regenerative dose D_r (L_r/T_r) is used for re-normalisation. Furthermore, although the difference in accuracy between the two methods is less significant for given doses less than 210 Gy, the gSGC method is apparently more accurate for larger doses. Therefore, we recommend the use of gSGC method for future dating applications, when possible.

Acknowledgements

We thank both reviewers for their very extensive and thoughtful comments. The comments and suggestions of the reviewers have improved the manuscript significantly.

References

Adamiec, G., Heer, A.J., Bluszcz, A., 2012. Statistics of count numbers from a photomultiplier tube and its implications for error estimation. Radiat. Meas. 47 (9), 746–751.
Aitken, M.J., 1998. An Introduction to Optical Dating: the Dating of Quaternary Sediments by the Use of Photon-stimulated Luminescence. Oxford University Press, Oxford.
Bailey, R.M., 2001. Towards a general kinetic model for optically and thermally stimulated luminescence of quartz. Radiat. Meas. 33 (1), 17–45.
Bailey, R.M., 2004. Paper I-simulation of dose absorption in quartz over geological timescales and its implications for the precisionand accuracy of optical dating. Radiat. Meas. 38 (3), 299–310.
Bluszcz, A., Adamiec, G., Heer, A.J., 2015. Estimation of equivalent dose and its uncertainty in the OSL SAR protocol when count numbers do not follow a Poisson distribution. Radiat. Meas. 81, 46–54.
Burbidge, C.I., Duller, G.A.T., Roberts, H.M., 2006. De determination for young samples using the standardised OSL response of coarse-grain quartz. Radiat. Meas. 41 (3), 278–288.
Duller, G.A.T., 2008. Single-grain optical dating of Quaternary sediments: why aliquot size matters in luminescence dating. Boreas 37 (4), 589–612.
Duller, G.A.T., 2012. Improving the accuracy and precision of equivalent doses determined using the optically stimulated luminescence signal from single grains of quartz. Radiat. Meas. 47 (9), 770–777.
Feathers, J.K., Pagonis, V., 2015. Dating quartz near saturation-Simulations and application at archaeological sites in South Africa and South Carolina. Quat. Geochronol. 30, 416–421.
Galbraith, R.F., 1988. Graphical display of estimates having differing standard errors. Technometrics 30, 271–281.
Galbraith, R.F., 2002. A note on the variance of a background-corrected OSL count. Anc. TL 20 (2), 49–51.
Galbraith, R.F., Roberts, R.G., Laslett, G.M., Yoshida, H., Olley, J.M., 1999. Optical dating of single and multiple grains of quartz from Jinmium rock shelter, northern Australia: Part I, experimental design and statistical models. Archaeometry 41 (2), 339–364.
Jacobs, Z., Duller, G.A.T., Wintle, A.G., 2006. Interpretation of single grain De distributions and calculation of De. Radiat. Meas. 41 (3), 264–277.
Lai, Z.P., 2006. Testing the use of an OSL standardised growth curve (SGC) for De determination on quartz from the Chinese Loess Plateau. Radiat. Meas. 41 (1), 9–16.
Li, B., 2007. A note on estimating the error when subtracting background counts from weak OSL signals. Anc. TL 25 (1), 9–14.
Li, B., Roberts, R.G., Jacobs, Z., Li, S.H., 2015a. Potential of establishing a 'global standardised growth curve' (gSGC) for optical dating of quartz from sediments. Quat. Geochronol. 27, 94–104.
Li, B., Roberts, R.G., Jacobs, Z., Li, S.H., Guo, Y.J., 2015b. Construction of a 'global standardised growth curve' (gSGC) for infrared stimulated luminescence dating of K-feldspar. Quat. Geochronol. 27, 119–130.
Long, H., Lai, Z.P., Fan, Q.S., Sun, Y.J., Liu, X.J., 2010. Applicability of a quartz OSL standardised growth curve for De determination up to 400 Gy for lacustrine sediments from the Qaidam Basin of the Qinghai-Tibetan Plateau. Quat. Geochronol. 5 (2–3), 212–217.
Murray, A.S., Olley, J.M., 2002. Precision and accuracy in the optically stimulated luminescence dating of sedimentary quartz: a status review. Geochronometria 21, 1–16.
Murray, A.S., Wintle, A.G., 2000. Luminescence dating of quartz using an improved single-aliquot regenerative-dose protocol. Radiat. Meas. 32 (1), 57–73.
Pagonis, V., Adamiec, G., Athanassas, C., Chen, R., Baker, A., Larsen, M., Thompson, Z., 2011a. Simulations of thermally transferred OSL signals in quartz: accuracy and precision of the protocols for equivalent dose evaluation. Nucl. Instrum. Meth. Phys. Res. B 269 (12), 1431–1443.
Pagonis, V., Baker, A., Larsen, M., Thompson, Z., 2011b. Precision and accuracy of two luminescence dating techniques for retrospective dosimetry: SAR-OSL and SAR-ITL. Nucl. Instrum. Meth. Phys. Res. B 269 (7), 653–663.
Pagonis, V., Balsamo, E., Barnold, C., Duling, K., McCole, S., 2008. Simulations of the predose technique for retrospective dosimetry and authenticity testing. Radiat. Meas. 43 (8), 1343–1353.
Pagonis, V., Chen, R., Kitis, G., 2011c. On the intrinsic accuracy and precision of luminescence dating techniques for fired ceramics. J. Archaeol. Sci. 38 (7), 1591–1602.
Pagonis, V., Chen, R., Wintle, A.G., 2007a. Modelling thermal transfer in optically stimulated luminescence of quartz. J. Phys. D. Appl. Phys. 40 (4), 998–1006.
Pagonis, V., Kitis, G., Furetta, C., 2006. Numerical and Practical Exercises in Thermoluminescence. Springer Science and Business Media, New York.
Pagonis, V., Wintle, A.G., Chen, R., 2007b. Simulations of the effect of pulse annealing on optically-stimulated luminescence of quartz. Radiat. Meas. 42 (10), 1587–1599.
Peng, J., Dong, Z.B., Han, F.Q., Long, H., Liu, X.J., 2013. R package numOSL: numeric routines for optically stimulated luminescence dating. Anc. TL 31 (2), 41–48. http://CRAN.R-project.org/package=numOSL.
Peng, J., Pagonis, V., 2016. Simulating comprehensive kinetic models for quartz luminescence using the R program KMS. Radiat. Meas. 86, 63–70. https://github.com/pengjunUCAS/KMS.
Roberts, H.M., Duller, G.A.T., 2004. Standardised growth curves for optical dating of sediment using multiple-grain aliquots. Radiat. Meas. 38 (2), 241–252.
Shen, Z.X., Mauz, B., 2011. Estimating the equivalent dose of late Pleistocene fine silt quartz from the Lower Mississippi Valley using a standardized OSL growth curve. Radiat. Meas. 46 (8), 649–654.
Stevens, T., Armitage, S.J., Lu, H.Y., Thomas, D.S.G., 2007. Examining the potential of high sampling resolution OSL dating of Chinese loess. Quat. Geochronol. 2 (1–4), 15–22.
Telfer, M.W., Bateman, M.D., Carr, A.S., Chase, B.M., 2008. Testing the applicability of a standardized growth curve (SGC) for quartz OSL dating: Kalahari dunes, South African coastal dunes and Florida dune cordons. Quat. Geochronol. 3 (1–2), 137–142.
Thomsen, K.J., Murray, A.S., Bøtter-Jensen, L., 2005. Sources of variability in OSL dose measurements using single grains of quartz. Radiat. Meas. 39 (1), 47–61.
Truscott, A.J., Duller, G.A.T., Bøtter-Jensen, L., Murray, A.S., Wintle, A.G., 2000. Reproducibility of optically stimulated luminescence measurements from single grains of Al_2O_3:C and annealed quartz. Radiat. Meas. 32 (5–6), 447–451.
Wintle, A.G., 2008. Fifty years of luminescence. Archaeometry 50 (2), 276–312.
Yang, L.H., Lai, Z.P., Long, H., Zhang, J.R., 2011. Construction of a quartz OSL standardised growth curve (SGC) for aeolian samples from the Horqin dunefield in Northeastern China. Geochronometria 38 (4), 391–396.